The XXII LNF Spring School "Bruno Touschek"

9th Young Researchers Workshop

Istituto Nazionale di Fisica Nucleare

The New ATLAS pixel detector for the High Luminosity LHC

Beka Buadze

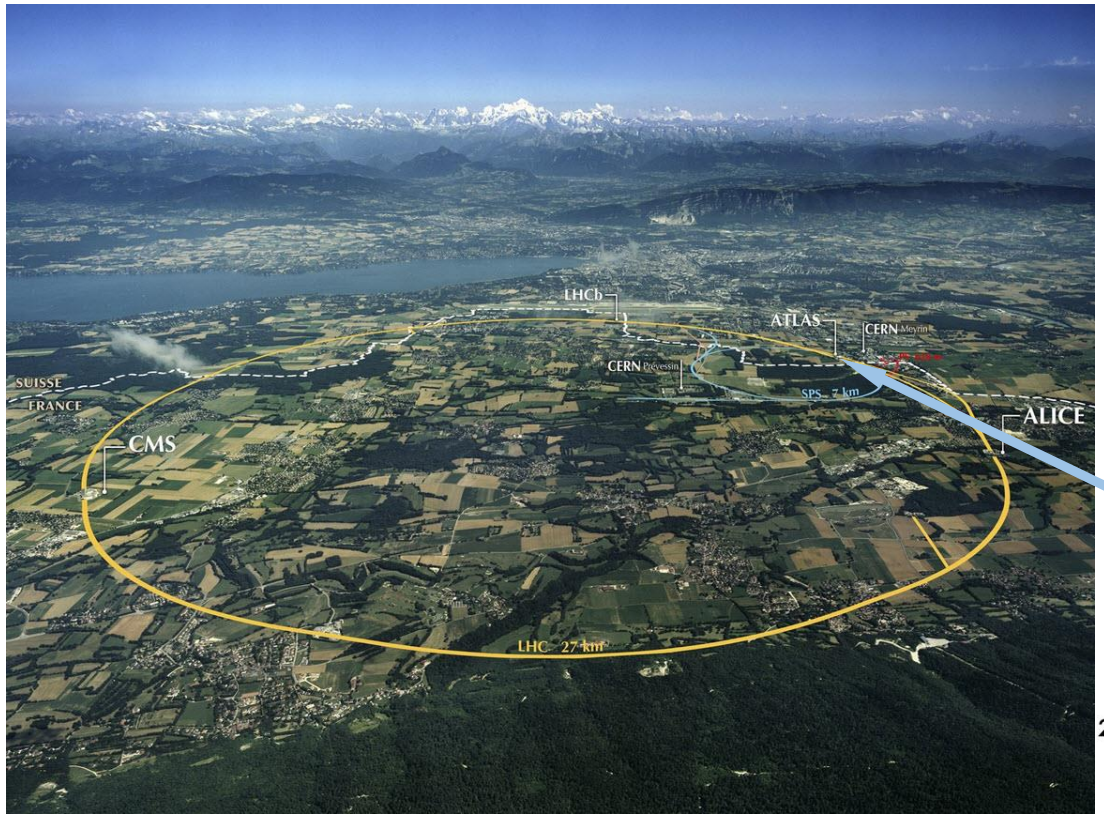

The Large Hadron Collider (LHC) is the world's largest and most powerful particle accelerator. It is 27 km in circumference and located about 100 meters underground. The LHC hosts four main experiments: ATLAS, CMS, ALICE, and LHCb.

Current LHC (Run 3)

- Proton-proton collisions with center-of-mass energies up to **13.6 TeV**.
- Average collisions per bunch crossing:
$$\langle \mu \rangle \sim 40\text{–}60$$
- Integrated luminosity collected so far:
$$\int Ldt \sim 300\ fb^{-1}$$

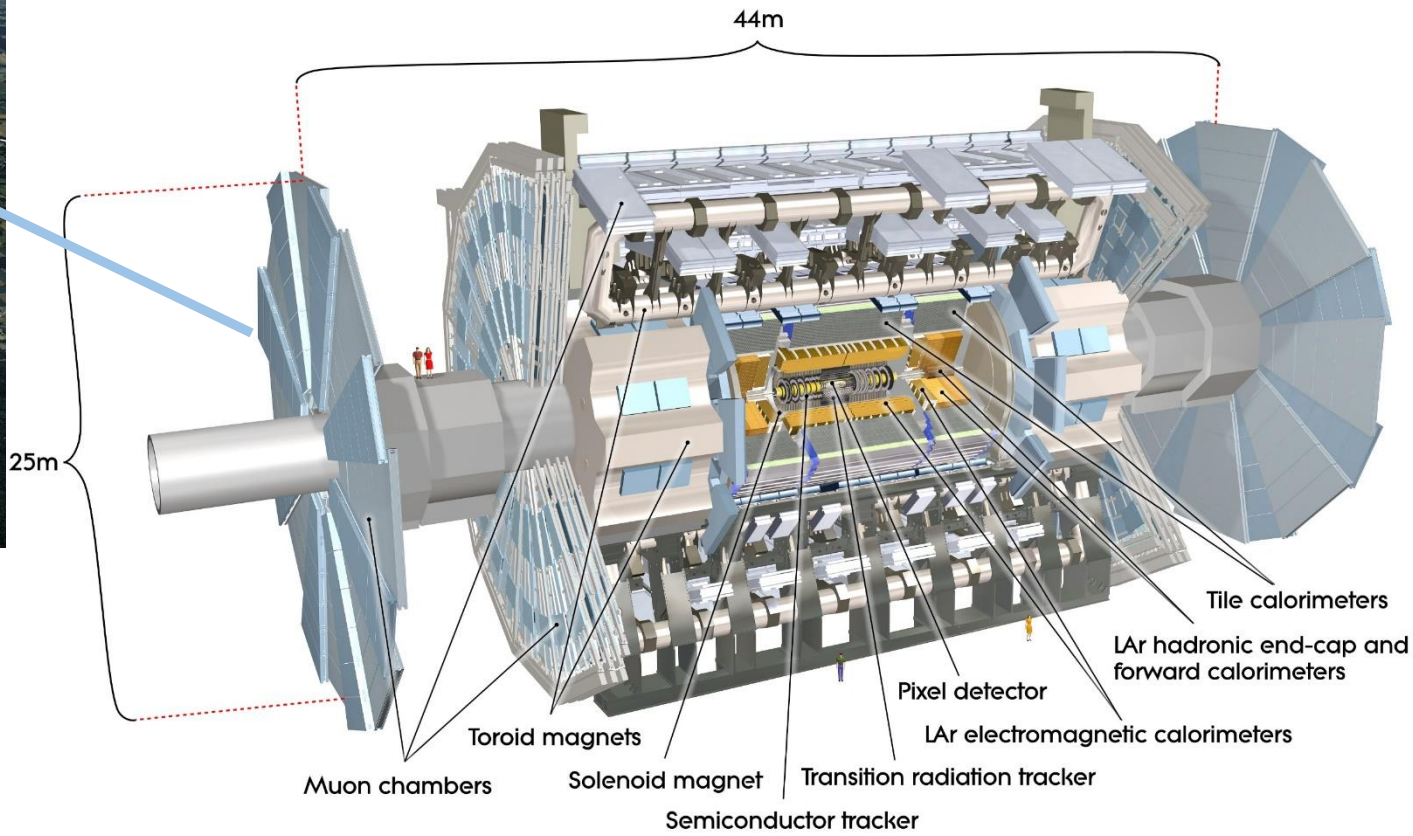

LHC / HL-LHC Plan

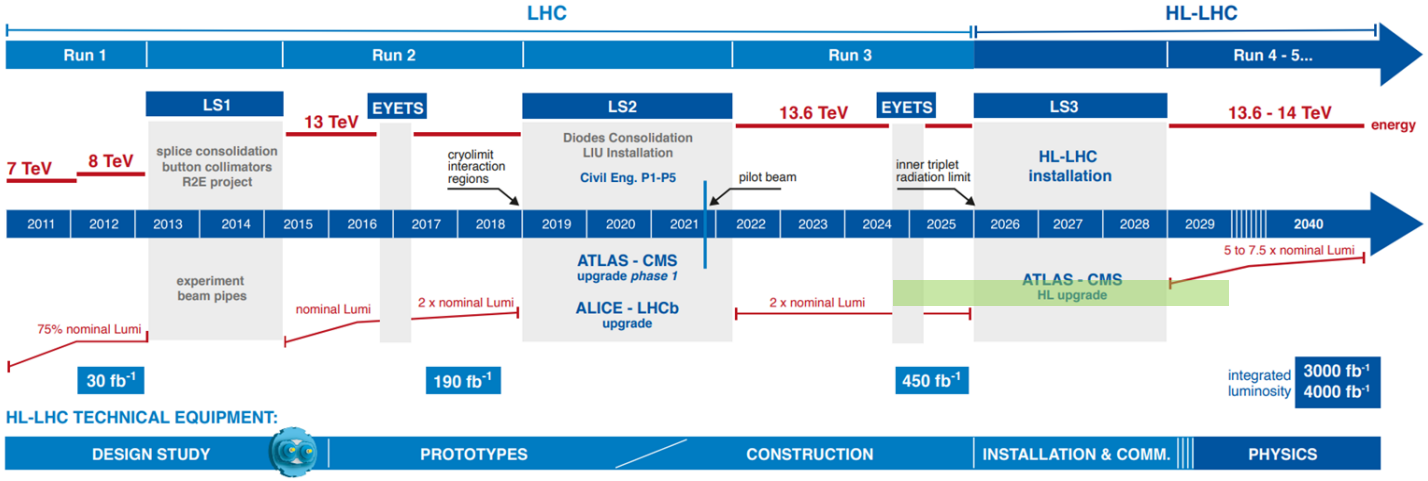

Scientific Goals

- Study the properties of the Higgs boson with higher precision
- Search for new particles and phenomena beyond the Standard Model

LHC : 19 -55
Pile up
events

HL-LHC: 140 -200
Pile up events

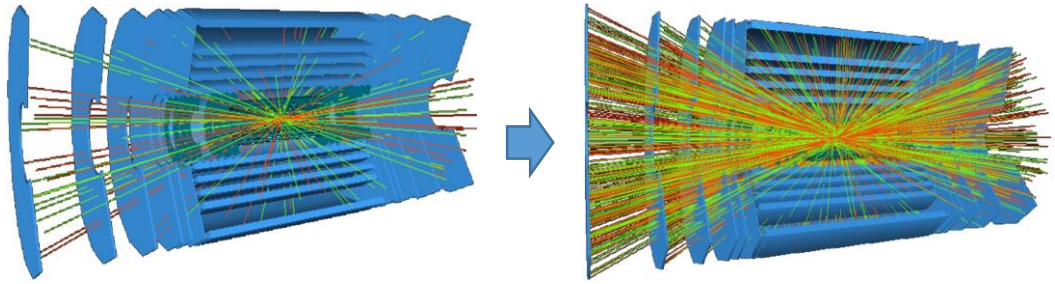

HL-LHC Conditions (from 2029)

- Proton–proton collisions at center-of-mass energies up to 14 TeV
- Average interaction bunch crossing increased from:

$$\langle\mu\rangle\sim40 \rightarrow \langle\mu\rangle\sim200 \text{ (high pile-up conditions)}$$

- Integrated luminosity:

$$\int Ldt \sim 4000\ fb^{-1}$$

approximately ten times larger than the current dataset

- Instantaneous luminosity increased by a factor of 5–7.5 above the nominal value:

$$1\times10^{34} cm^{-2} s^{-1}$$

Consequences for the Detector

- Increased particle density → need for higher detector granularity and improved track separation
- Higher trigger rates → need for faster readout and data processing systems
- Increased radiation damage → need for more radiation-hard detector technologies and materials

ITk sub Detectors

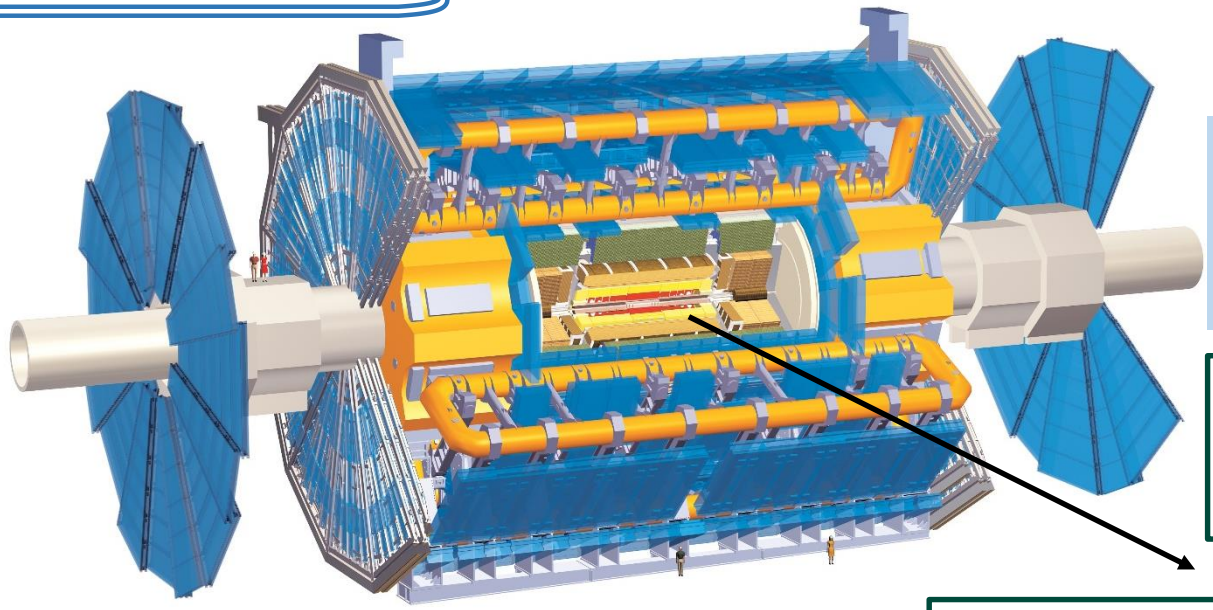

ITk Upgrade

- Designed to maintain or improve tracking performance in the HL-LHC environment
- Completely redesigned all-silicon tracking detector
- Includes 5 inner pixel layers and 4 outer strip layers
- Pseudorapidity coverage extended to |η|<4, more than 9 hits per track

ITk Strip Barrel Structure

The ITk includes strip barrel structures located in the central cylindrical region of the detector, surrounding the beam axis. It covers the central region up to approximately |η| < 2.5

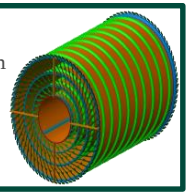

ITk Strip Endcap Structure

The ITk includes two endcap structures positioned at both ends of the detector, perpendicular to the beam axis, covering the forward regions with 1.6 < |η| < 2.7

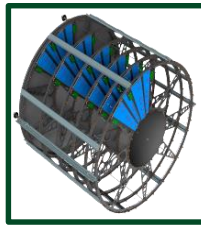

ITk Pixel Inner Endcap Structure

The ITk includes inner pixel endcap structures positioned at both ends of the detector, perpendicular to the beam axis, covering the forward regions with 2.0 < |η| < 3.6

Inner Endcap rings

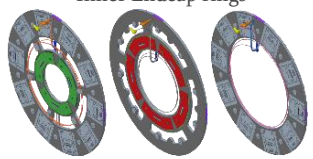

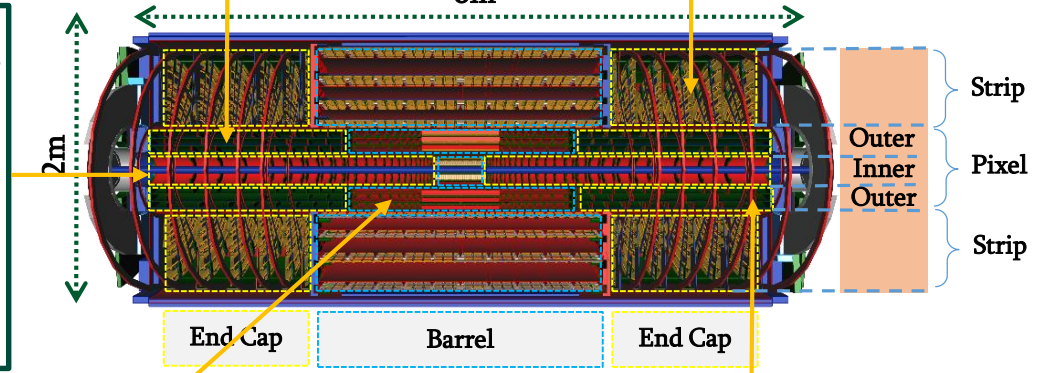

Atlas Inner Tracker

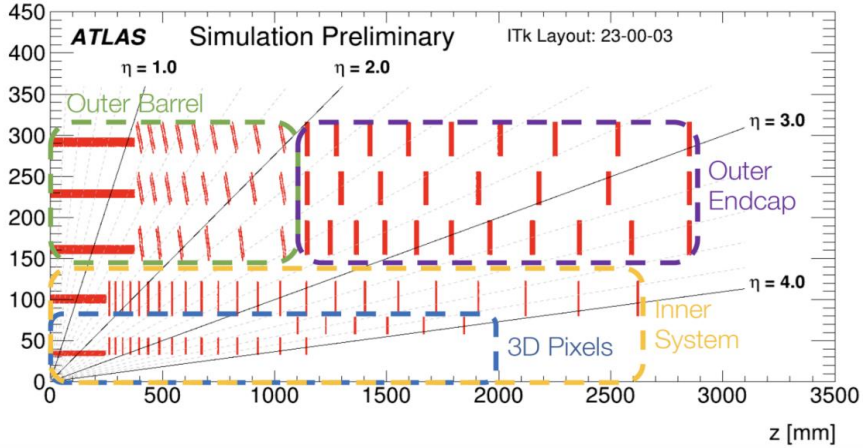

ITk Pixel Outer Barrel Structure

The ITk includes a pixel outer barrel structure located in the central cylindrical region of the detector, surrounding the beam axis. It covers the central region up to approximately |η| < 2.0

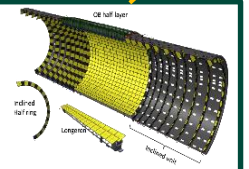

ITk Pixel Outer Endcap Structure

The ITk includes outer pixel endcap structures located at both ends of the detector, perpendicular to the beam axis. These structures cover the forward regions with 1.6 < |η| < 2.9

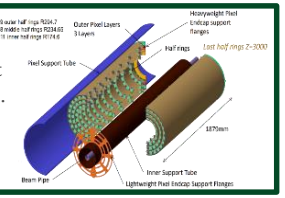

Atlas ITK Pixel Outer End-Cap

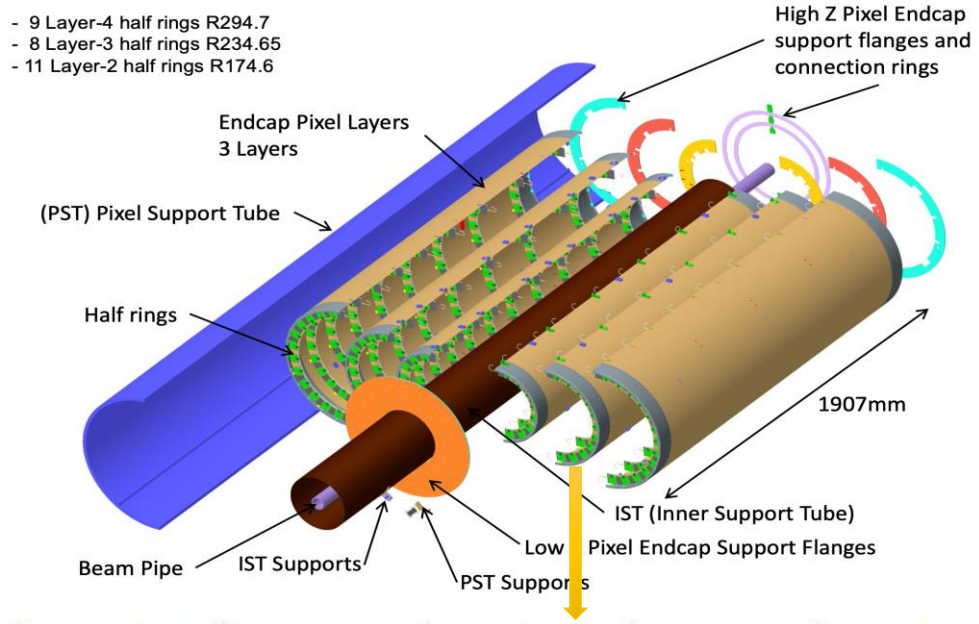

- Pixel detectors provide high efficiency (>97%) at high radiation doses exceeding $10^{16} n_{eq}/cm^2$ under HL-LHC conditions
- The ATLAS ITk Pixel Outer End-Cap is composed of carbon half-rings mounted on both sides of the detector. The structure includes L2, L3, and L4 half-rings, supporting 16, 22, and 26 silicon pixel modules, respectively. Each half-shell contains 11 L2, 8 L3, and 9 L4 half-rings,

pixel detector module

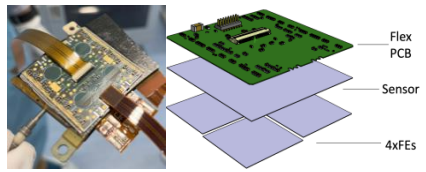

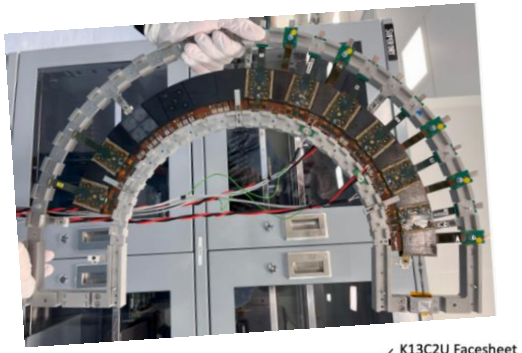

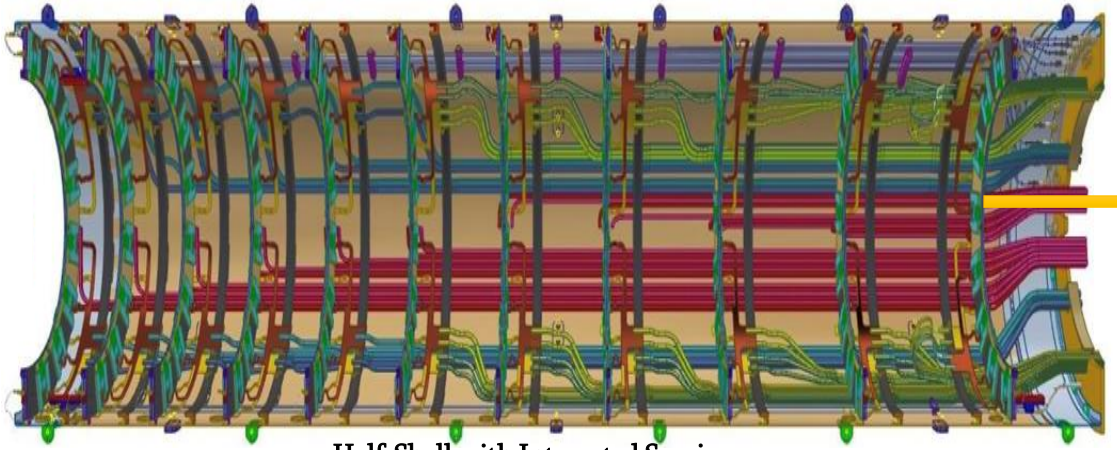

Half-Shell with Integrated Services

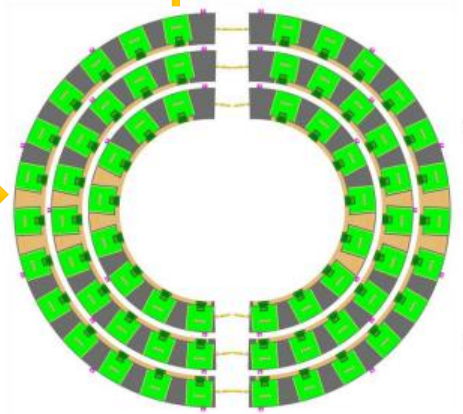

L2/L3/L4 Half-Rings with Sensors

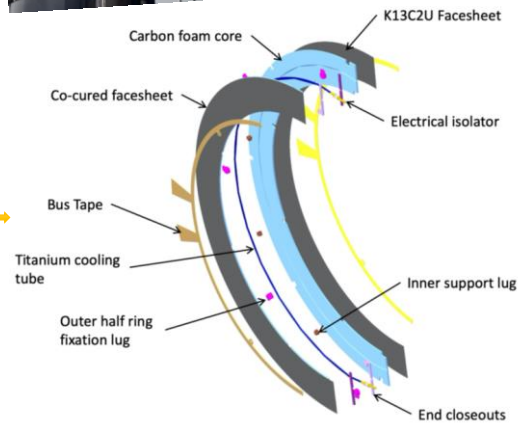

Half-Ring Structure

OEC Materials and Properties

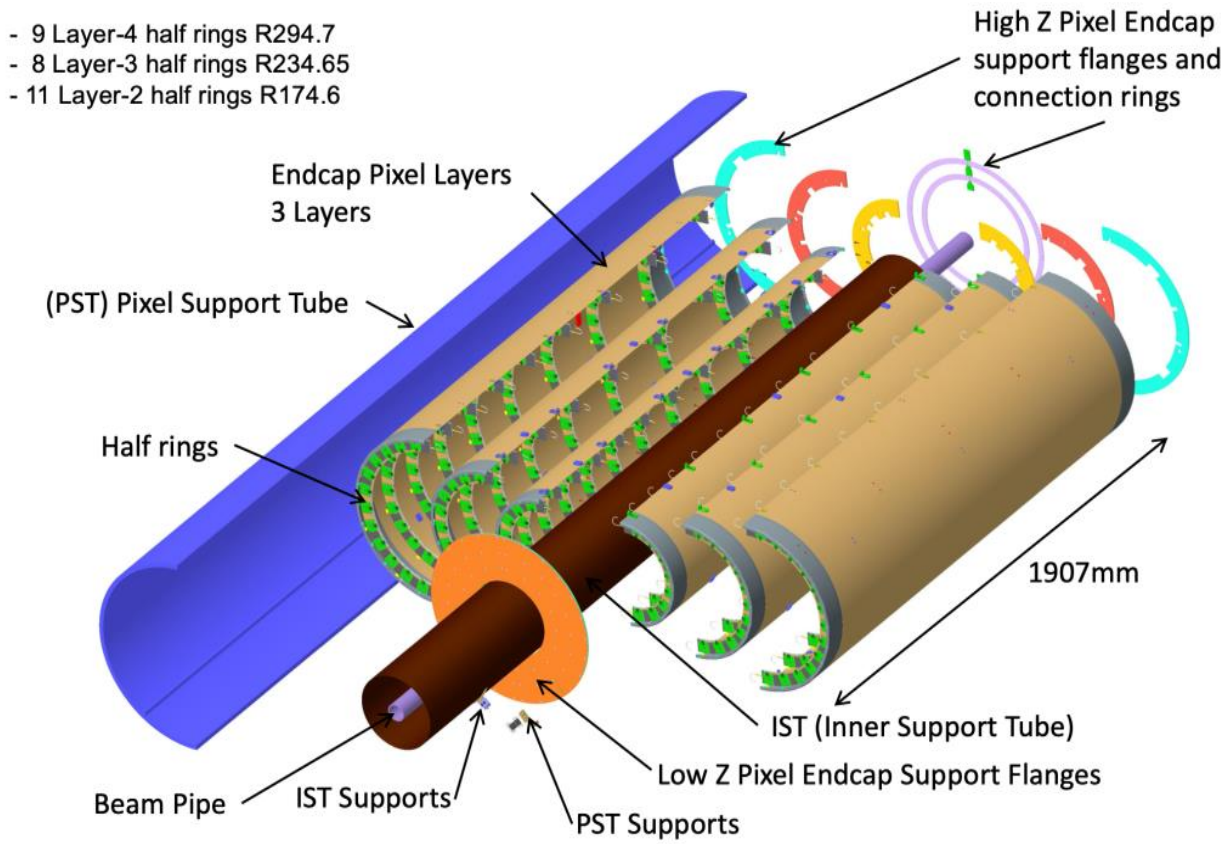

Material choice is important because charged particles undergo multiple Coulomb scattering while passing through matter.
This effect causes:

- track distortion
- reduced momentum precision

The rms scattering angle is described by the Lynch–Dahl formula:

$$Q_0=\frac{13.6\ \text{MeV}}{\beta cp} z \sqrt{\frac{x}{X_0}}[1+0.038\ \ln(\frac{xz^2}{X_0\beta^2})] \Rightarrow Q_0 \sim \sqrt{\frac{x}{X_0}}$$

less material → less multiple scattering → better tracking precision

Material	Application	Young's Modulus	CTE (10^{-6}/°C)
CFRP M55J/EX-1515	Global Structures (Shells, Flanges)	~259 GPa	1.05 to 34.7
CFRP K13C2U/EX-1515	Half-Rings Facings	~259 GPa	-0.71
Titanium Grade 2	Inserts, Cooling Pipes, Fittings	105 GPa	8.6
ULTEM 1000	Interlinks, Mounting Lugs	3.2 GPa	50.0
Nomex Honeycomb	Radial Support Core	0.12 GPa	34.9

Detector Operating Temperature Range

- Detector lifetime: approximately 100 cooling–heating cycles
- Operating temperature range:

$$-45°C \leq T \leq +40\ °$$

- Defined by the CO_2 cooling and detector safety systems.

Facility and some mesurment tools

Frascati Facility

Assembling Trolley

Climate Chamber

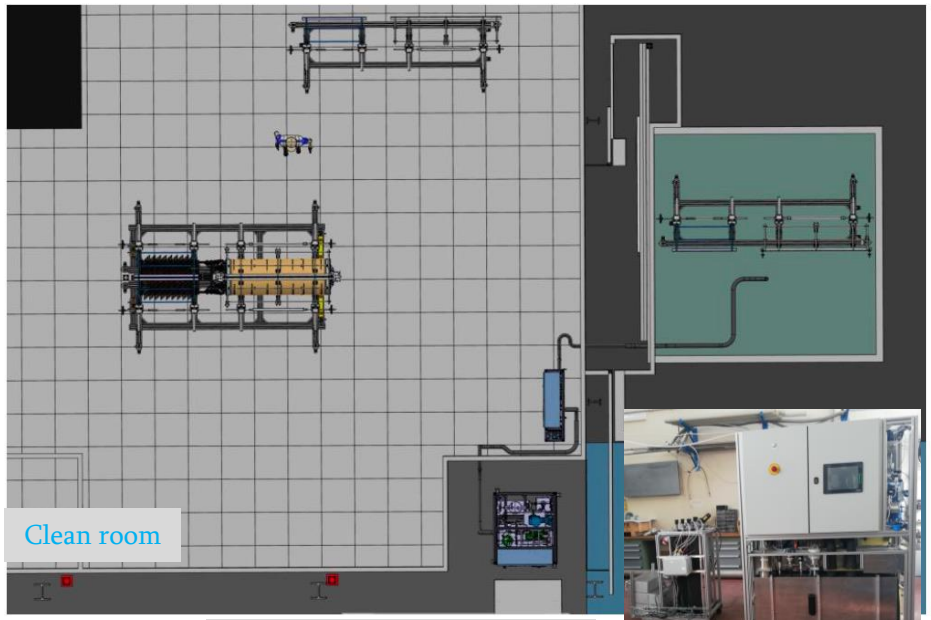

Clean room

LUCASZ CO_2 Cooling System

strain gauge

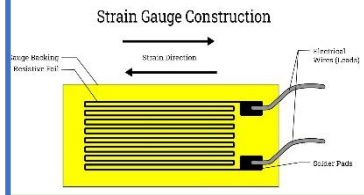

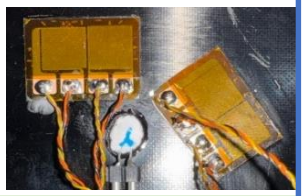

A strain gauge works on the principle that when a material is stretched or compressed, its electrical resistance changes.

The strain gauge is attached to a surface, so it deforms together with the material.

By measuring the change in resistance, we can calculate the amount of strain or force applied.

Two common methods:

1. Absolute Distance Meter (ADM)

measures the absolute distance directly by sending a modulated laser beam to a reflector and comparing the phase shift of the returned signal. This allows the tracker to know the exact position of the target.

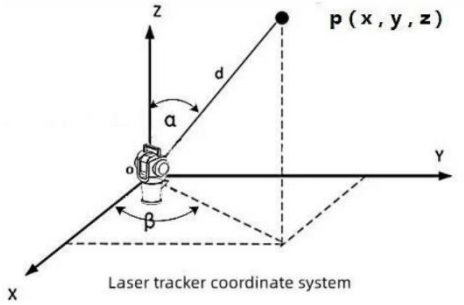

2. Interferometer (very high precision)

measures very small displacement changes by splitting a laser beam into a reference beam and a measurement beam. When the beams recombine, they create interference fringes. By counting the fringes, the system calculates movement with extremely high accuracy.

Measurement of radial support

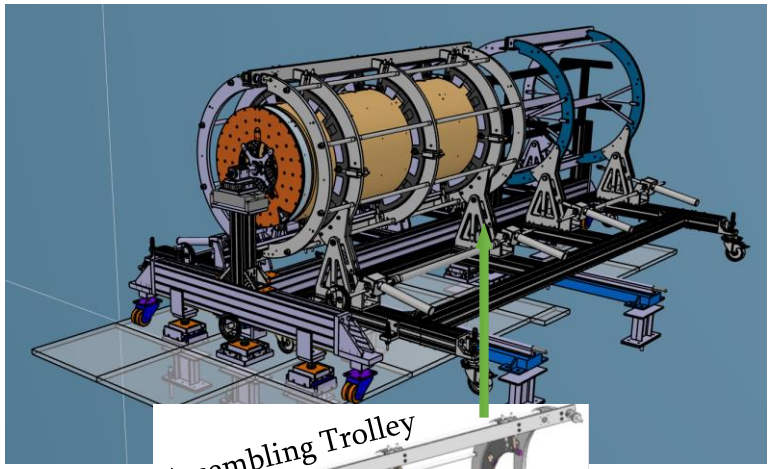

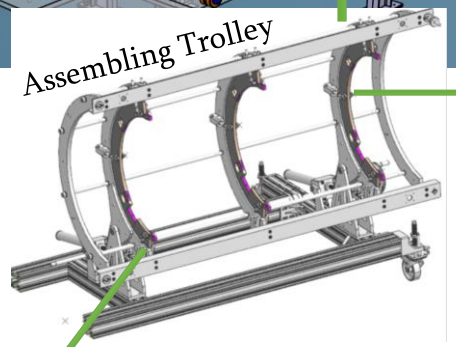

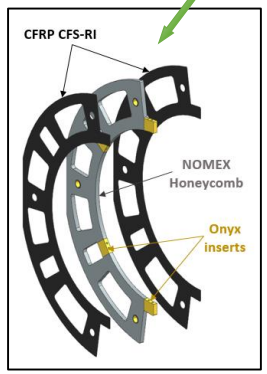

- The radial support holds the inner tracker assembly on the trolley during assembly
- The radial support is a sandwich structure with FRP CFS-RI outer skins of 1.0 mm thickness and a Nomex Honeycomb ANC-4.8-48 (OX) core.
- Additionally, Onyx inserts are used at the connection points where the structure is attached to other structural elements.

FEM model

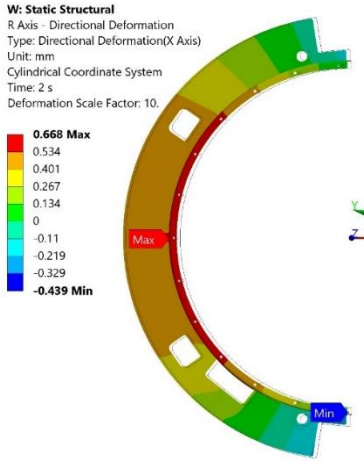

Radial deformation
UR_{max} = 0.67 mm

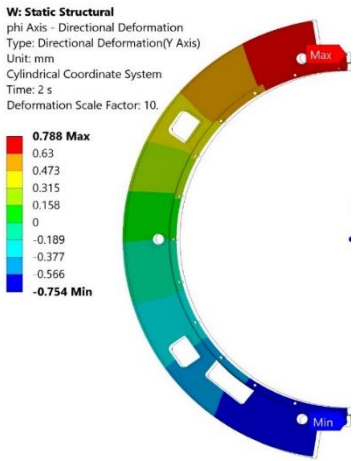

rPHI deformation
$UrPHI_{max}$ = 0.79 mm

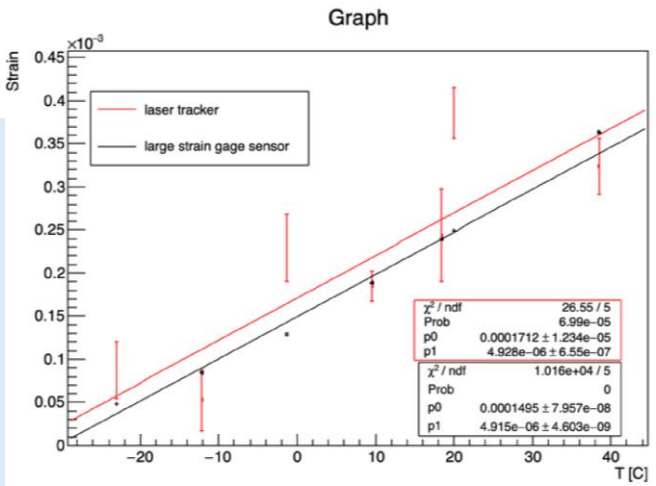

The radial support underwent a thermal cycle inside the chamber. Strain gage data were corrected using Zerodur reference data and provider specifications. The estimated CTE was 5.6 ppm/°C (4.9 ppm/°C in the second case), in good agreement with the laser tracker measurements.

The measurements showed an expansion of **0.4 mm**, which is in good agreement with the simulation results. In the simulation

Half-Shell Thermal Cycling

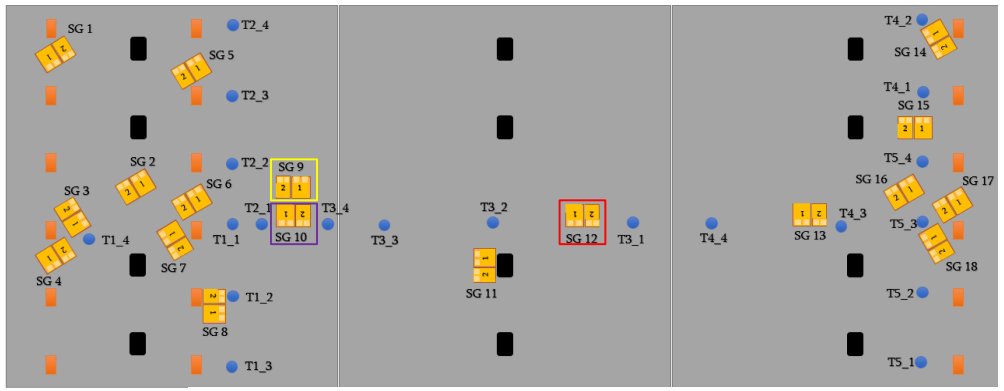

STR_9 STR_10 STR_12

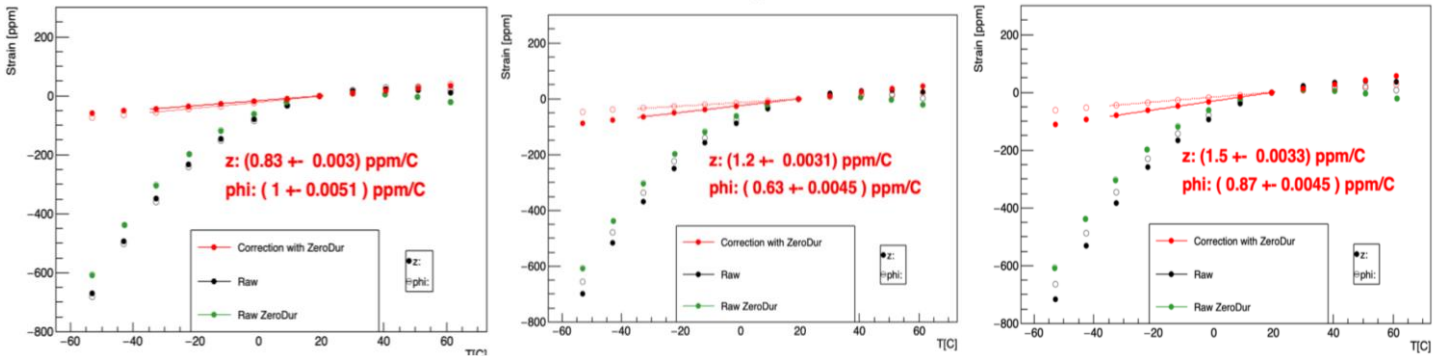

Graph Graph Graph

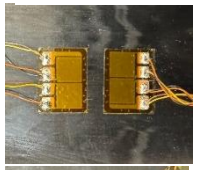

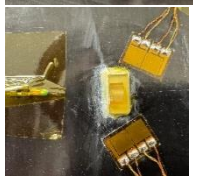

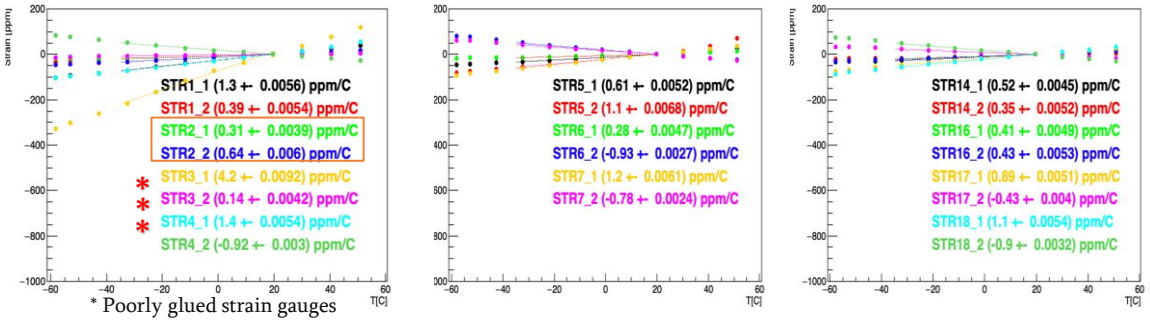

* Poorly glued strain gauges

Radial deformation of the L4 half-shell
FEM model: empty L4 half-shell

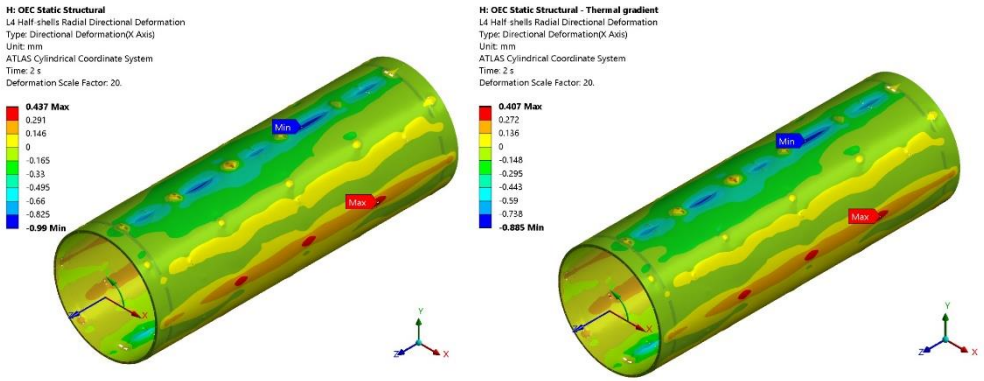

- The FEA simulations were used to identify the regions of the L4 half-shell characterized by high thermo-mechanical deformation and strong deformation gradients.
- Based on the radial deformation maps, the strain gauges were positioned in the most critical regions for the experimental investigation.

- The FEA simulations predicted high thermo-mechanical deformation around the lugs and interlink regions.
- Therefore, strain gauges were installed in these critical areas to monitor the local structural response during thermal cycling.
- The measurements remained within a safe range throughout the tests.
- A visual inspection performed after 11 thermal cycles showed no cracks, delamination, or glue debonding

Summary

- The new ATLAS ITk detector is being developed for the HL-LHC, where the number of particles, radiation levels, and pile-up events will be much higher than in the current detector.
- To work in these difficult conditions, the detector needs new engineering solutions, radiation-resistant silicon sensors, lightweight carbon materials, and modern cooling systems to keep good tracking performance and high precision.
- Accurate deformation measurements, thermal tests, and metrology systems are also very important to guarantee stable and reliable detector operation during long-term use in extreme experimental conditions.

INFN
Istituto Nazionale di Fisica Nucleare

Thank You For Your Attention!

TOR VERGATA
UNIVERSITÀ DEGLI STUDI DI ROMA

9th Young Researchers Workshop

13.05.2026

ATLAS EXPERIMENT

Backup Slides

Upgrade ID Tracker to ITk

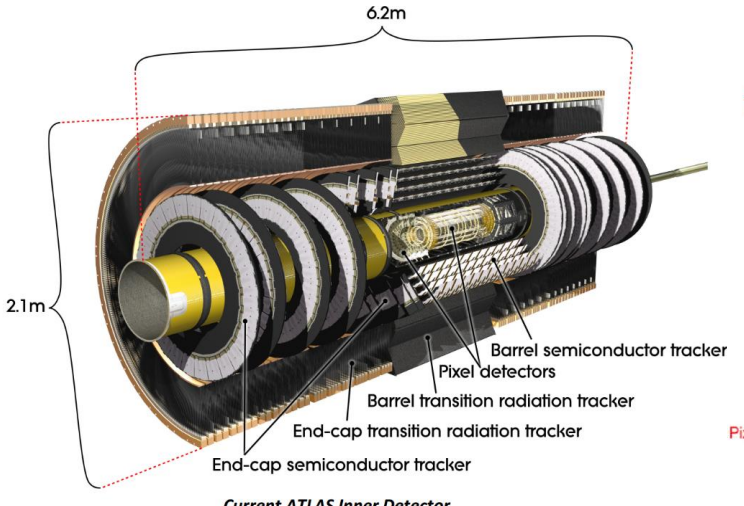

Current ATLAS Inner Detector

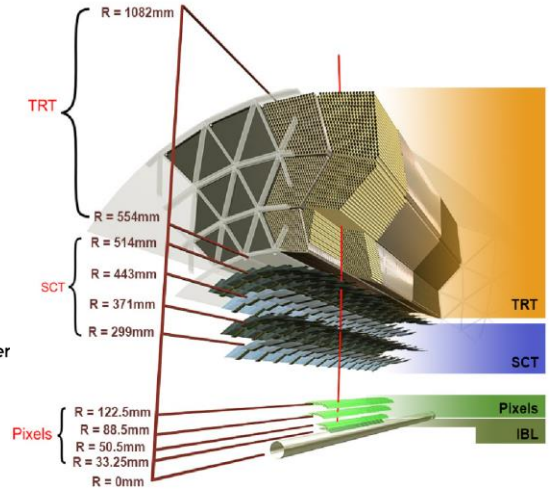

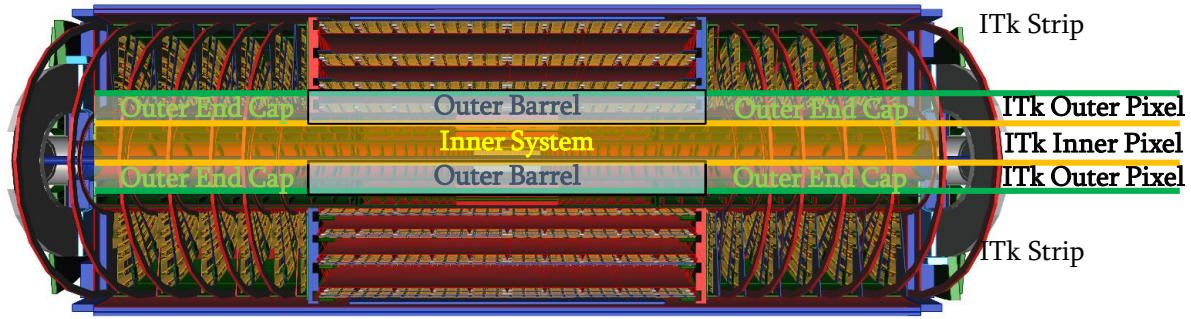

ID vs ITk layout

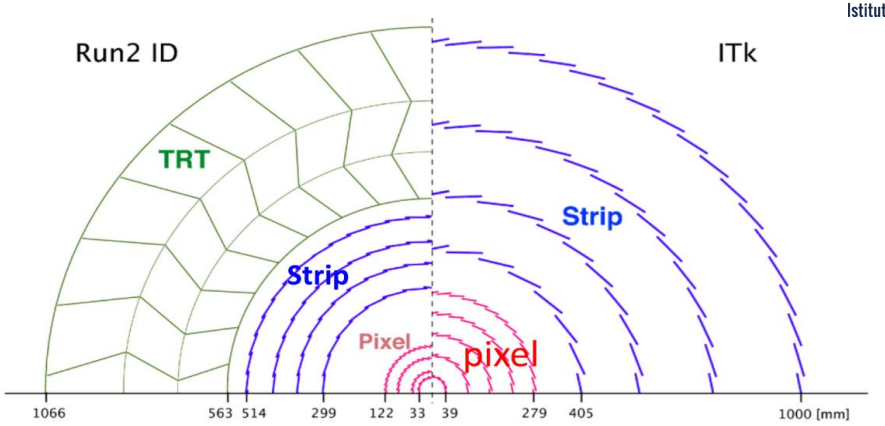

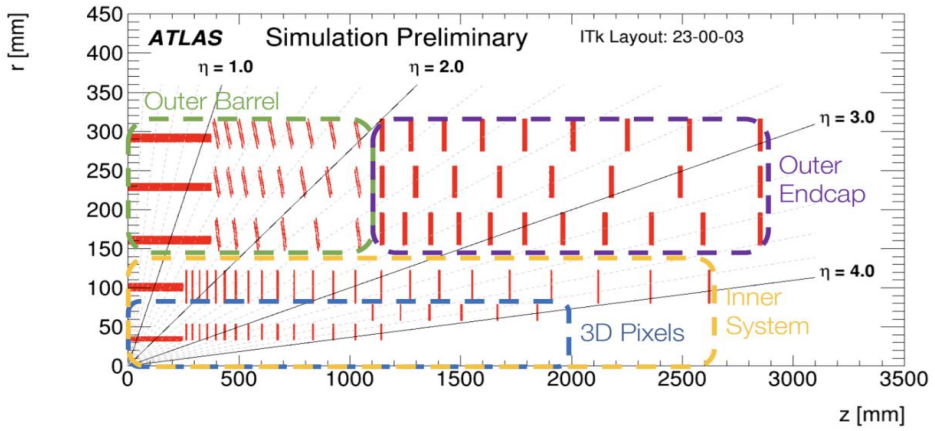

ITk (ID)	Area (m^2)	# Modules	# Channels (M)	Pseudo-rapidity $\|\eta\|$	Instantaneous luminosity (L)	Integrated luminosity ($\int Ldt$)
Pixels	~13 (1.9)	~9700 (2000)	~5100 (92)	<4 (<2.5)	7×10^{34} $cm^{-2}s^{-1}$ (1×10^{34} $cm^{-2}s^{-1}$)	4000 fb^{-1} (300 fb^{-1})
Strips	~165 (61)	~17888 (4088)	~60 (6.3)			

Climate Chamber

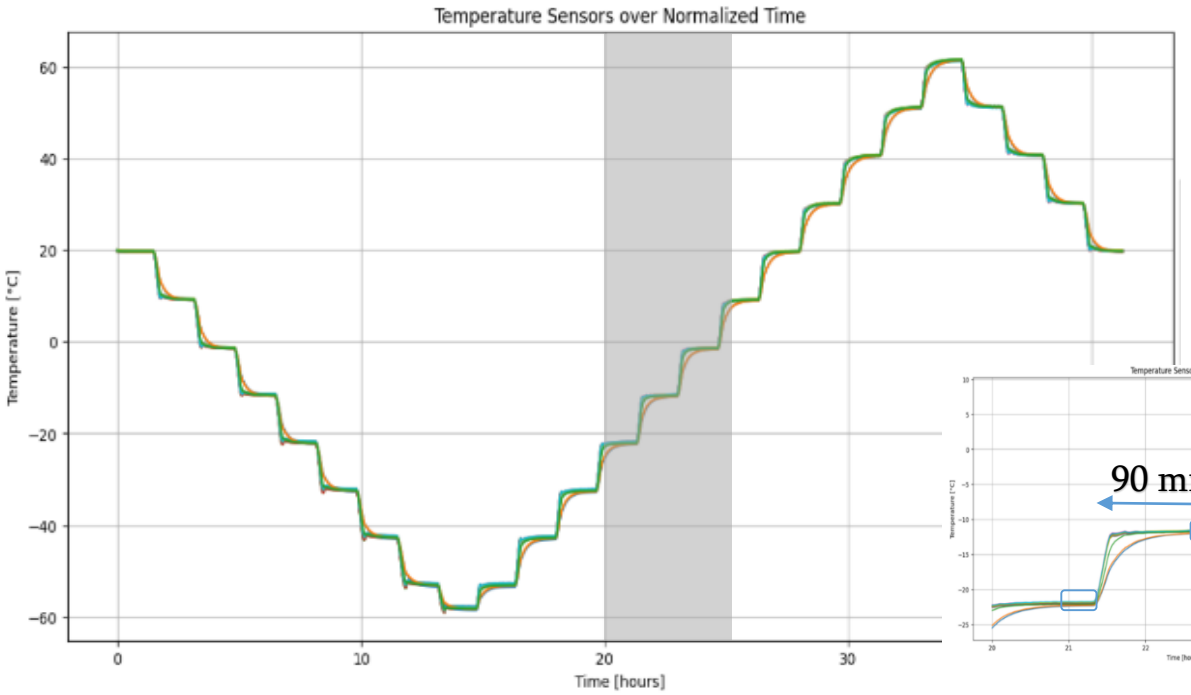

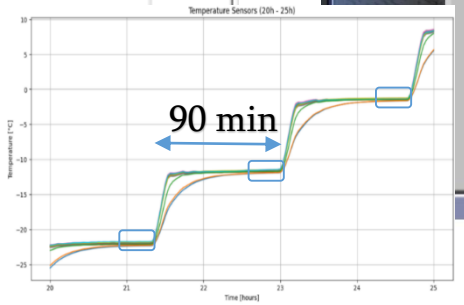

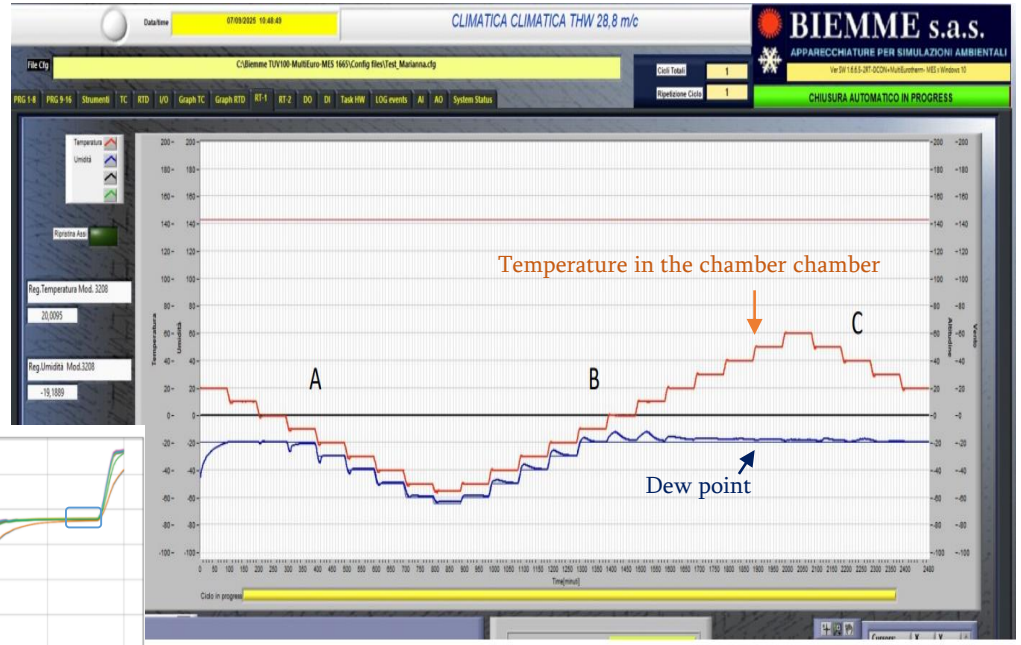

- The thermal cycle begins by cooling from +20 °C down to -55 °C, then heating up to +60 °C. After that, the temperature returns to +20 °C.
- Each step was 10 °C and was changed every 90 minutes, which was required for temperature saturation
- In total, the complete thermal cycle takes approximately 43 hours.

The graph highlights the zones where the temperature is stable, and measurements from the sensors (LVDT, strain gauges) are taken.

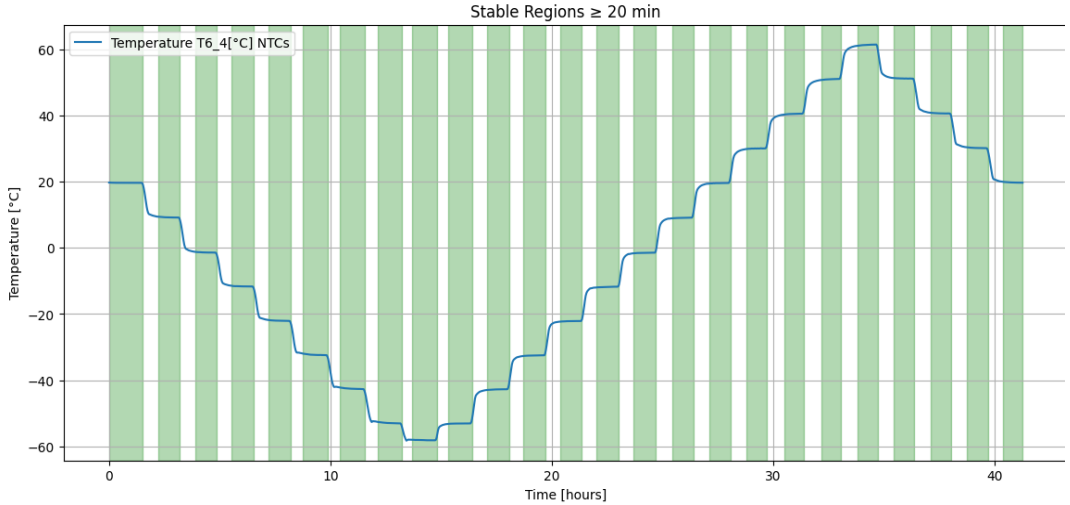

Visual inspection of HS mounting Lugs

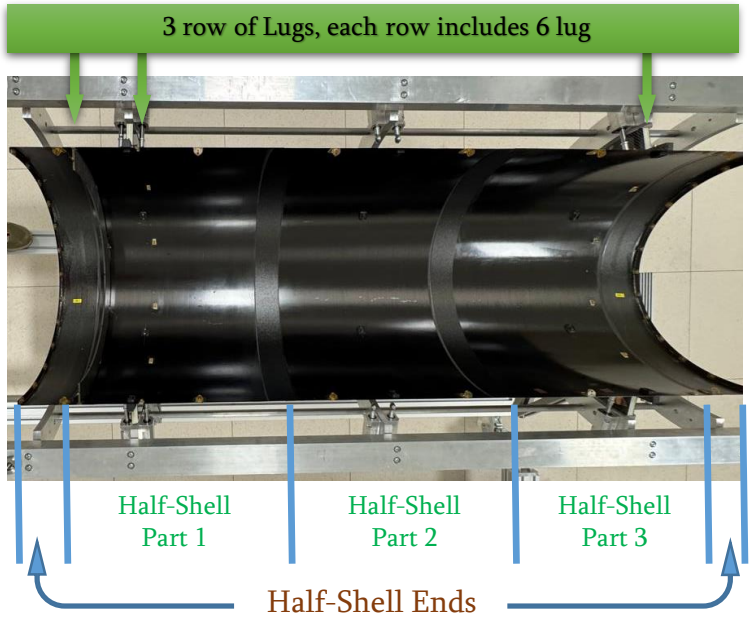

The lugs are made of ULTEM material and are attached to the inner surface of the carbon half-Shell. These lugs serve as holders for the half-rings, on which the pixel detectors are mounted.

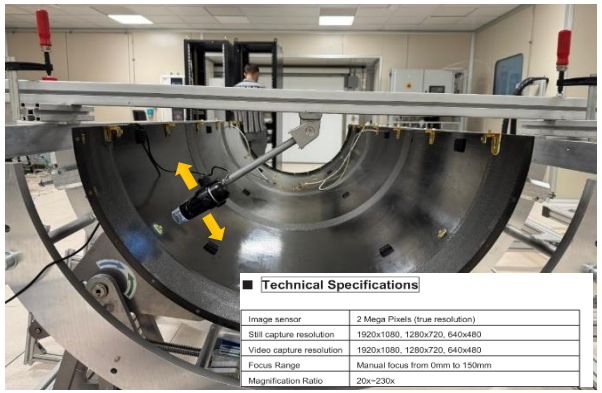

L2 – 4 lugs per half-ring
L3 – 5 lugs per half-ring
L4 – 6 lugs per half-ring

"Fiji (ImageJ) software used for detecting defects on the carbon surface of a half-shell under thermal cycling

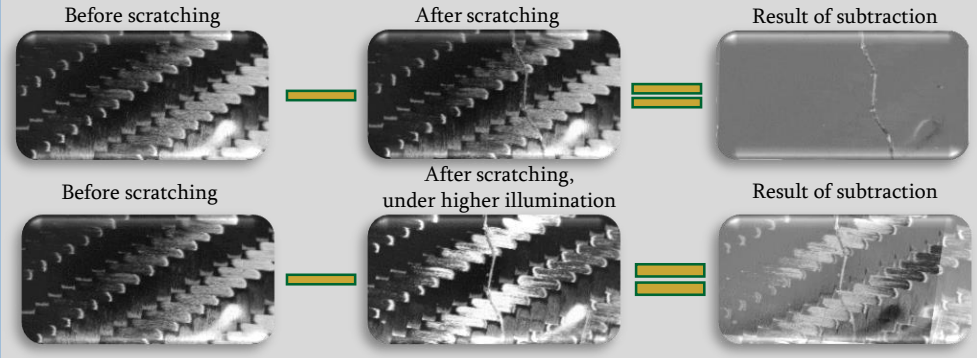

For visual inspection, microscope images were taken at the beginning of the thermal cycling, and the comparison is performed after the completion of the final cycle. A total of 13 thermal cycles were performed

13 thermal cycle (1)

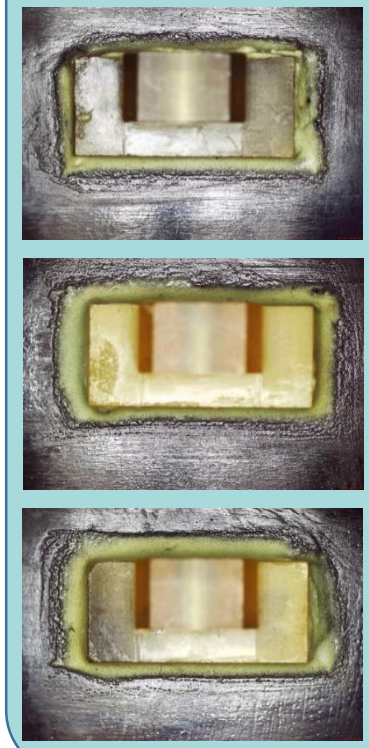

Before the first thermal cycle (2)

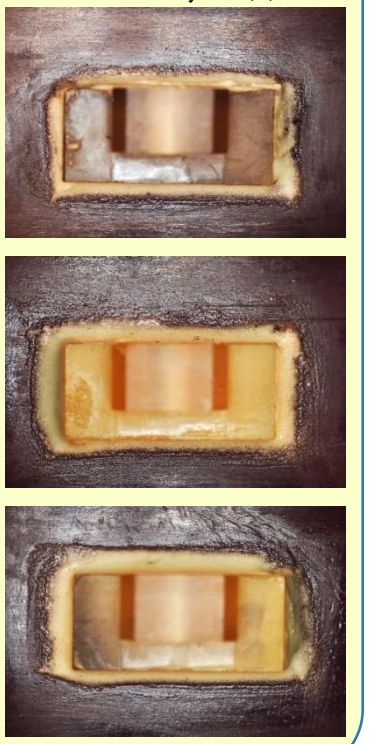

Subtract 1 from 2

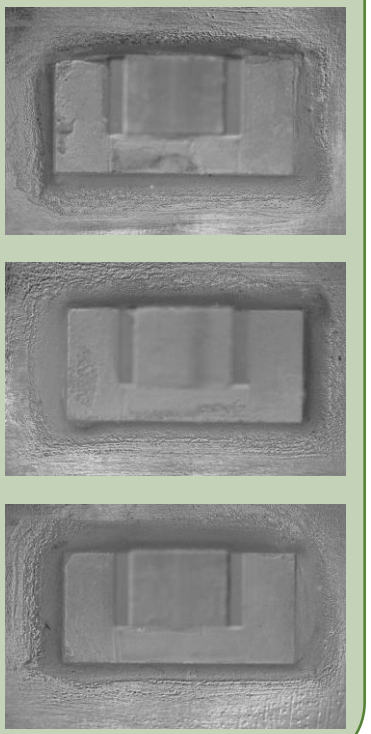

Visual inspection showed that after 13 thermal cycles (The thermal cycle begins by cooling from +20 °C down to -55 °C, then heating up to +60 °C. After that, the temperature returns to +20 °C), no damage was observed on the lugs - **no cracks, surface defects, or detachment** were detected

properties of radial support materials

INFN
Istituto Nazionale di Fisica Nucleare

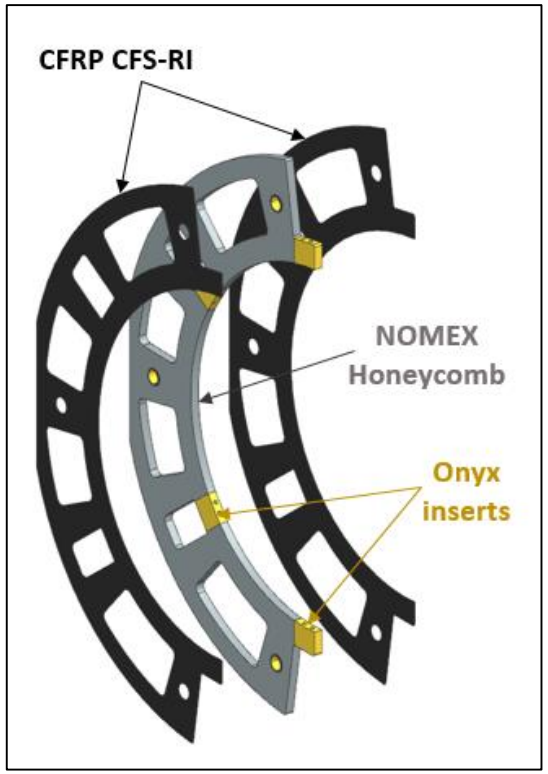

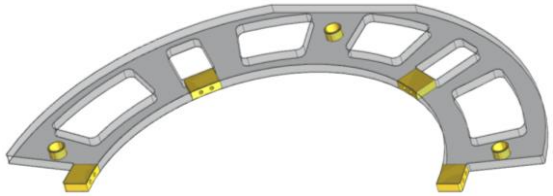

Note: Young Modulus and CTE depend on internal reinforcement, which are unknown. So, Young modulus of basic Onyx (2.4 GPa) and CTE 50 ppm/°C (conservative hypothesis) have been set as reference.

SCHEDA TECNICA DEL MATERIALE

Compositi

Markforged

Base composita	Prova (ASTM	Onyx	Onyx FR	Onyx ESD	Nylon
Modulo elastico (GPa)	D638	2,4	3,0	4,2	1,7
Tensione di snervamento (MPa)	D638	40	41	52	51
Tensione di rottura (MPa)	D638	37	40	50	36
Deformazione a rottura (%)	D638	25	18	25	150
Resistenza a flessione (MPa)	D790°	71	71	83	50
Modulo di flessione (GPa)	D790°	3,0	3,6	3,7	1,4
Temperatura di rammollimento a flessione (°C)	D648 B	145	145	138	41
Resistenza alla fiamma	UL94	—	V-0²	—	—
Prova d'urto di Izod - con intaglio (J/m)	D256-10 A	330	—	44	110
Resistività superficiale (Ω	ANSI/ESD STM11.11³	—	—	10⁸ - 10¹¹	—
Densità (g/cm³)	—	1,2	1,2	1,2	1,1

Fibre continue	Prova (ASTM)	Carbonio	Carbon FR	Kevlar®	Fibra di vetro	HSHT FG
Resistenza a trazione (MPa)	D3039	800	760	610	590	600
Modulo elastico (GPa)	D3039	60	57	27	21	21
Deformazione a rottura (%)	D3039	1,5	1,6	2,7	3,8	3,9
Resistenza a flessione (MPa)	D790°	540	540	240	200	420
Modulo di flessione (GPa)	D790°	51	50	26	22	21
Deformazione in flessione a rottura (%)	D790°	1,2	1,6	2,1	1,1	2,2
Resistenza a compressione (MPa)	D6641	420	300	130	180	216
Modulo di compressione (GPa)	D6641	62	59	25	24	21
Deformazione in compressione a rottura (%)	D6641	0,7	0,5	1,5	—	0,8
Temperatura di rammollimento a flessione (°C)	D648 B	105	105	105	105	150
Prova d'urto di Izod - con intaglio (J/m)	D256-10 A	960	810	2000	2600	3100
Densità (g/cm³)	—	1,4	1,4	1,2	1,5	1,5

markforged.com REV 5.2 - 20/01/2022 480 Pleasant St. Watertown, MA 02472

Nomex Honeycomb ANC-4.8-48(OX)
E_c = 120 MPa
CTE = 34.9 x 10^{-6}/°C

TYPICAL APPLICATIONS
- Racing car bodywork
- Ground antennas and radomes
- Marine applications—ranging from interior panels, flooring, hatches
- Leisure applications—skis and surfboards
- Precision optical equipment
- Filter systems

PRODUCT DESIGNATION

e.g.	ANC (a)	4.8 (b)	48 (c)	(OX) (d)
a. ANC	Nomex® commercial honeycomb			
b. 3.2	Cell size in millimeters			
c. 29	Density (kg/m³)			
d. (OX)	Overexpanded			

PRODUCT RANGE

Standard products:
The following products are usually available as ex-stock items. Additional grades can be sourced upon request, subject to minimum order quantities and extended lead times.
- ANC-3.2-48
- ANC-4.8-32
- ANC-4.8-48

STANDARD DIMENSIONS AND TOLERANCES

Nominal sheet length (W) = 2500 ± 75 mm
Nominal sheet width (L) = 1250 ± 75 mm
Sheet thickness as requested from 1.5 mm to 100 mm ± 0.125 mm
Sheet thickness above 100 mm, tolerance = ± 0.25
Density as nominal ± 10%

Nomex® Honeycomb
Commercial Grade

TORAY
Toray Advanced Composites

PRODUCT DATA SHEET

MECHANICAL PROPERTIES

Property	Stabilized Compression		Plate Shear			
	Strength (MPa)	Modulus (MPa)	Strength "L Direction" (MPa)	Modulus "L Direction" (MPa)	Strength "W Direction" (MPa)	Modulus "W Direction" (MPa)
ANC-3.2-48	2.17	127	1.10	36	0.62	21
ANC-4.8-32	1.20	75	0.70	29	0.40	19
ANC-4.8-48	2.40	140	1.20	40	0.70	25
ANC-4.8-48(OX)	2.90	120	0.76	22	0.49	43

HEXAGONAL CELL

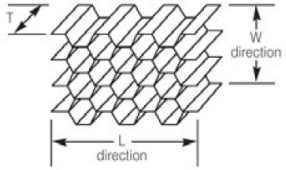

OVEREXPANDED CELL

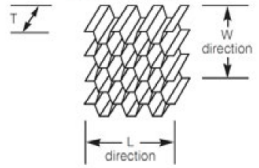

T = Thickness or cell depth L = Ribbon direction W = Direction perpendicular to the ribbon direction

CFRP CFS-RI: thickness 1.0 mm
E_c = 32.4 GPa
CTE = 4.94 x 10^{-6}/°C (see next slide)

easycomposites

Technical Datasheet
CFS-RI
High Strength Carbon Fibre Sheet

Key Features
- 100% high strength carbon fibre
- Flat, textured bonding surface on reverse

Description

Premium quality carbon fibre sheet manufactured using 100% high-strength carbon fibre reinforcement and epoxy resin with a smooth, glossy, cosmetic quality carbon fibre finish on one side and a textured 'peel-ply' finish on the reverse.

Typical Uses
- Motorsport / marine / light aircraft
- Engineering / automation
- Displays / exhibitions / shop-fitting
- Cabinets / enclosures / high-end audio
- Further processing into sandwich panels

Specification

Quasi-Isotropic Layup

To create a more uniform distribution of strength, these sheets are manufactured using layers of 0°/90° and 45°/-45° oriented reinforcement in a quasi-isotropic fibre orientation. This offers improved stiffness across their diagonal axis and significantly improved torsional stiffness.

Laminate Composition and Tolerances

Using a high temperature cure cycle to maximise mechanical strength, the sheets also have a resultant Tg (glass transition temperature) of 80°C.

To achieve maximum stability and flatness the sheets are made with a symmetrical stack up in both fibre weight and weave.

Sheet Thickness	Layup Schedule	Thickness & Tolerance
1.0mm	210g 22 twill 300g +/-45 biax 210g 22 twill	0.9mm +/- 0.2mm
2.0mm	210g 22 twill 300g +/-45 biax 650g 22 twill 300g +/-45 biax 210g 22 twill	1.7mm +/- 0.2mm
3.0mm	210g 22 twill 300g +/-45 biax 650g 22 twill 210g 22 twill 650g 22 twill 300g +/-45 biax 210g 22 twill	2.8mm +/- 0.2mm
4.0mm	210g 22 twill 300g +/-45 biax 650g 22 twill 650g 22 twill 650g 22 twill 650g 22 twill 300g +/-45 biax 210g 22 twill	4.0mm +/- 0.2mm

Property	Units	Value*			
Sheet Thickness	mm	1.0	2.0	3.0	4.0
Weight	kg/m²	1.32	2.80	4.11	5.84
Density	g/cm³	1.15	1.02	1.27	4.46
Tensile Strength 0/90°	MPa	503	598	644	-
Tensile Strength 45°	MPa	557	622	443	-
Tensile Modulus 0/90°	GPa	37.2	43.9	47.4	-
Tensile Modulus 45°	GPa	32.3	34.5	27.1	-
Youngs Modulus 0/90° Gloss Side Compr.	GPa	32.4	35.1	10.3	-
Youngs Modulus 0/90° Gloss Side Tension	GPa	31.6	35.3	10.5	-
Elongation at Break at 0/90°	%	2.27	2.91	3.88	-
Elongation at Break at 45°	%	3.13	4.11	4.10	-

*Data measured from a typical production sheet

Materials properties used in the Pixel OEC

PART	MATERIAL	Density [Kg/m^3]	Young's Modulus [GPa]			Poisson's ratio			Shear Modulus [GPa]			CTE [1e^{-6}/°C]			Ref. Temperature [°C]
			X (1)	Y (2)	Z (3)	XY (12)	YZ (23)	XZ (13)	XY (12)	YZ (23)	XZ (13)	X (1)	Y (2)	Z (3)	
Half-rings: facings	CFRP K13C2U/EX-1515 [0/90/0] V.f. 48.9%	1645	295.52	150.51	150.51	0.0117	0.0117	0.0117	5.3	5.3	5.3	-0.713	0.153	0.153	
Half-rings: carbon foam	Lockeed Martin K9 δ=0.40 g/cm^3	400	0.2931			0.33						1.0			
Half Rings: cooling pipe & fittings VEE/Flat sliders Front support: inserts	Titanium GR2	4500	105			0.34						8.6			
Half Rings: electrical breaker	Ceramic 97.6% Alumina	3760	340			0.22						6.9			
Half-rings: bus tape v.6	Orthotropic Laminate Copper/Kapton	4805	53.06	53.06	53.06	0.34	0.34	0.34	19.8	19.8	19.8	18.2	18.2	18.2	
Half-rings: lugs/closeouts Interlinks/mounting lugs/spacers	ULTEM 1000	1270	3.2			0.36						50			20
L3/L4 Half-shells/end flanges L3/L4 Rear support Rear junctions and spokes C-rings of the electrical Type-1 services Saddle supports	CFRP M55J/EX-1515 $[90/45/-45/0]_S$, CFRP M55J/EX-1515 $[90/45/-45/0]_{10S}$ CFRP M55J/EX-1515 $[90/45/-45/0]_{5S}$ V.f. 46.5% (all)	1514	89.85	89.85	89.85	0.324	0.324	0.324	33.92	33.92	33.92	0.261	0.261	0.261	
Front support: core	CF HONEYCOMB CORE UCF-306-1/4-6.0	32	4.83E-01	4.83E-01	4.83E-01	0.3	0.3	0.3	0.0048	0.0048	0.0048	4.5			
IST	CFRP K13C2U/EX-1515 $[0/90/0]_{2S}$ V.f. 48.9%	1645	152.98	152.98	152.98	0.319	0.319	0.319	57.97	57.97	57.97	-0.419	-0.419	-0.419	
L2 Half-shells/end flanges Front support: facings	Pre-preg MJ55/EX1515, Vf. 46.5%, 80 gsm, CPT 75 µm Ref.: [9], [11], EsaComp	1514	258.97	4.4917	4.4917	0.25	0.27	0.25	2.4661	1.773	2.4661	-1.05	61	61	
L2 Rear support												-1.05	34.7	34.7	-55

- Half-shell made in MJ55/EX1515 [90/45/-45/0] are based on UD Pre-Preg MJ55/EX1515; Vf:46.5%; 80gsm; CPT 75 µm.